AIRBORNE MONITORING OF VEHICLE ACTIVITY IN URBAN AREAS

U. Stilla [a] *, E. Michaelsen [b], U. Soergel [b], S. Hinz [c], J. Ender[d]

[a] Photogrammetry and Remote Sensing, Technische Universitaet Muenchen, 80290 Muenchen, Germany
[b] FGAN-FOM Research Institute for Optronics and Pattern Recognition, 76275 Ettlingen, Germany
[c] Remote Sensing Technology, Technische Universitaet Muenchen, 80290 Muenchen, Germany
[d] FGAN-FHR Research Institute for High Frequency Pysics and Radar Techniques, 53343 Wachtberg, Germany

stilla@bv.tum.de

Commission III, WG III/4

KEY WORDS: Urban, Monitoring, Aerial, Infrared, SAR

ABSTRACT:

In this paper several possibilities of vehicle extraction from different airborne sensor systems are described. Three major frequency domains of remote sensing are considered, namely (i) visual, (ii) thermal IR and (iii) radar. Due to the complementing acquired scene properties, the image processing methods have to be tailored for the peculiarities of the different kinds of sensor data. (i)Vehicle detection in aerial images relies upon local and global features. For modelling a vehicle on the local level, a 3D-wireframe representation is used describing prominent geometric and radiometric features of cars including their shadow region. A vehicle is extracted by a "top-down" matching of the model to the image. On the global level, vehicle queues are modelled by ribbons that exhibit typical symmetries and spacing of vehicles over a larger distance. Fusing local and global extractions makes the result more complete. (ii) Particularly at night video sequences from an infrared camera yield suitable data to assess the activity of vehicles. At the resolution of approximately one meter vehicles appear as elongated spots. However, in urban areas many additional other objects have the same property. Vehicles may be discriminated from these objects either by their movement or by their temperature and their appearance in groups. Using map knowledge as context, a grouping of vehicles into rows along road margins is performed. (iii) The active scene illumination and large signal wavelength of SAR allows remote sensing on a day-night basis and under bad weather conditions. High-resolution SAR systems open the possibility to detect objects like vehicles and to determine the velocity of moving objects. Along-track interferometry allows estimation even small vehicle movements. However, in urban areas SAR specific illumination phenomena like foreshortening, layover, shadow, and multipath-propagation burden the interpretation. Particularly the visibility of the vehicles in inner city areas is in question. A high resolution LIDAR DEM is incorporated to determine the visibility of the roads by a SAR measurement from a given sensor trajectory and sensor orientation. Shadow and layover areas are detected by incoherent sampling of the DEM. In order to determine the optimal flight path a large number of simulations are carried out with varying viewing and aspect angles.

1. INTRODUCTION

Traffic monitoring in dense build-up areas is a complex issue. Research on this topic is motivated from different fields of application: Traffic-related data play an important role in urban and spatial planning, e.g., for road net optimization and for estimation or simulation of air and noise pollution. Furthermore, because of the growing amount of traffic, research on car detection is also motivated by the strong need to automate the traffic flow management by intelligent control and guidance systems. The management of big events or the emergencies after a disaster may require up-to-date traffic information. This is important, e.g., to assess the parking situation or to find ways for a task force into a danger zone when crowds try to escape from this zone. Other fields of application are found in the context of military reconnaissance and extraction of geographical data for Geo Information Systems (GIS), e.g., for site model generation and up-date.
The White Paper on the Common Transport Policy (2001) of the European Communities has identified congestion, pollution and energy consumption as key causes for the deteriorating performance of Europe's transport systems, especially in the industrialised urban regions. The 6th European Frame Program providing a budget of EUR 610 million for "Sustainable Surface Transport" emphasizes the importance of traffic monitoring and the demand on research. Some objectives are environmentally friendly transport systems, safety improvement and traffic congestion avoidance.
Automatic surveillance, planning, or control of traffic requires data of the actual traffic situation. Stationary inductive or optical sensors provide a permanent but only local measurement of the traffic situation. Space borne sensors allow a spatial measurement, but usually with low repetition rate and degree of flexibility. Airborne systems can be used flexibly for data recording of areas or routes. Depending on the task (e.g. traffic census, measurement of traffic density or velocity, vehicle discrimination, vehicle activity) different passive or active sensors could be appropriate for the monitoring. For example, investigations on congestion for a special route section have been done with a video camera mounted on a helicopter [Gorte et al, 2002] or vehicle discrimination in LIDAR data has been studied [Toth et al., 2003]

In this paper, several possibilities to extract vehicles from data of three frequency domains are described, namely (i) visual, (ii) thermal IR and (iii) radar. Corresponding to the data, different processing methods are demanded.

* Corresponding author (stilla@bv.tum.de).

2. VISUAL DATA

In recent years, attempts have been made to derive traffic data also from aerial images, because such images belong to the fundamental data sources in many fields of urban planning. Therefore, an algorithm that automatically detects and counts vehicles in aerial images would effectively support traffic-related analyses in urban planning.

2.1 Related work

Related work on vehicle detection from optical images can be distinguished based on the underlying type of modeling used: Several authors propose the use of an appearance-based, implicit model [Ruskoné et al., 1996], [Rajagopalan et al., 1999] [Schneidermann & Kanade, 2000], [Papageorgiou & Poggio, 2000]. The model is created by example images of cars and typically consists of grayvalue or texture features and their statistics assembled in vectors. Detection is then performed by computing the feature vectors from image regions and matching them against the statistics of the model features. The other group of approaches incorporates an explicit model that describes a vehicle in 2D or 3D, e.g., by a filter or wire-frame representation [Burlina et al., 1995], [Tan et al., 1998], [Haag & Nagel, 1999], [Liu et al.; 1999], [Liu, 2000], [Michaelsen & Stilla, 2000], [Zhao & Nevatia, 2001], [Hinz & Baumgartner, 2001], [Moon et al., 2002]. In this case, detection relies on either matching the model "top-down" to the image or grouping extracted image features "bottom-up" to construct structures similar to the model. If there is sufficient support of the model in the image, a vehicle is assumed to be detected.

2.2 Vehicle model

For detecting single vehicles an explicit model is used. Geometrically, a car is modelled as a 3D object by a wire-frame representation containing substructures like windshield, roof, and hood (see Fig. 1). An accurate computation of the car's shadow projection derived from date, daytime, and image orientation parameters is added to the model. As a radiometric feature, color constancy between hood color and roof color is included.

A detailed description requires a large number of models to cover all types of vehicles. To overcome this problem a tree-like model hierarchy is used having a simple 3D-box model at its root from which all models of higher level of detail can be derived subsequently.

2.3 Detection of single vehicles

The detection of single vehicles can be summarized by the following steps: (i) Extract edge pixels and compute gradient direction using Deriche's filter (ii) Project the geometric model including shadow region to edge pixel and align the model's reference point and direction with the gradient direction. The projection matrices are derived from the image orientation parameters. (iii) Measure reference color and intensity at roof region. (iv) Adapt the expected saliency of the edge features depending on position, orientation, color, and sun direction. (v) Measure features from the image: edge magnitude support of each model edge, edge direction support of each model edge, color constancy, darkness of shadow. (vi) Compute a matching score (a likelihood) by comparing measured values with expected values. (vii) Based on the likelihood, decide whether the car hypothesis is accepted or not. The evaluation measures

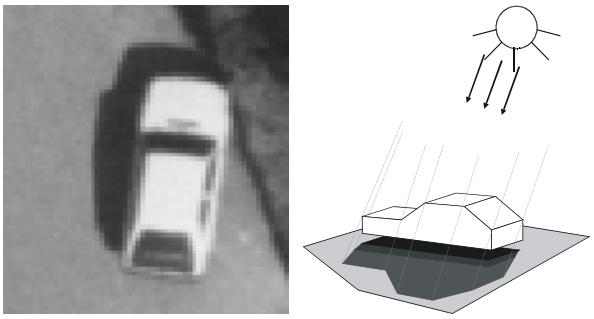

a b

Figure 1. Examples. a) Aerial image (section), b) Model involved are explained in [Hinz, 2004]. An example of detected vehicles is given in Fig. 2a.

2.4 Exploiting context

Due to the high geometric variability of vehicles, it can hardly be assured that the detailed model described above covers all types of vehicles. Only the contextual information that such a vehicle stands on a road or is part of a queue makes it clearly distinguishable from similar structures. For these reasons the queue model incorporates more generic and more global knowledge. Constraints of the detailed local model are relaxed and, in compensation for this, the global consistency of features is emphasized. More specifically, typical local geometric and radiometric symmetries of vehicles are exploited and, in combination with rough dimensions and spacings of vehicles, they are constrained to form an elongated structure ("ladder-like" shape) of sufficient length and smoothness. According to this model, vehicle queue detection is based on searching for one-vehicle-wide ribbons that are characterized by (i) significant directional symmetries of grayvalue edges with symmetry maxima defining the queue's center line, (ii) frequent intersections of short and perpendicularly oriented edges with homogeneous distribution along the center line, (ii) high parallel edge support at both sides of the center line and (iv) sufficient length. More details concerning the symmetry estimation are explained in [Hinz, 2004]

The results of the independent vehicle detection and queue detection are fused. A mutual overlap of vehicles and queues is checked and successfully tested vehicles are further investigated for collinearity with the queue's medial axis. After fusion the queues are analyzed for missing vehicles. Such vehicles are often characterized by homogenous blobs that can be extracted by a region-growing algorithm. In the last step, all vehicles detected using the stringent parametric model but not being part of a queue are added to the result.

a b

Figure 2. a) Result of the model match. b) Vehicles detected using local model (white) and vehicles recovered through fusion with global model (black)

3. THERMAL INFRARED DATA

3.1 Related work

Infrared sensors open the possibility of night vision and sensing the traffic situation by day and night. Vehicle movements can be captured by commercial IR-Cameras with a frame rate of 50 Hz (standard video out). An experimental airborne system including GPS and INS was built up within the LUMOS Project. It was shown that a tracking of moving objects exploiting the georefenced image sequence and map data is possible [Sujew & Ernst, 2003].

The activity of vehicles is not restricted to movement features alone. Stationary cars may still have the engine idling. They may be waiting at a traffic light or in a traffic jam. This is typical for rush hour situations in cities. Regarding e.g. pollution such cars have to be counted as active. Furthermore, for traffic management it might be helpful to distinguish cars that halt only for a short time - e.g. for loading, in a drive through service or just quickly picking things up - from those who are parked for hours or days. Temperature is an important feature for such recognition tasks. It is known that temperature can be remotely sensed by thermal cameras sensitive in the 3-5µm or 8-12µm spectral band [Wolffe & Zissis, 1985].

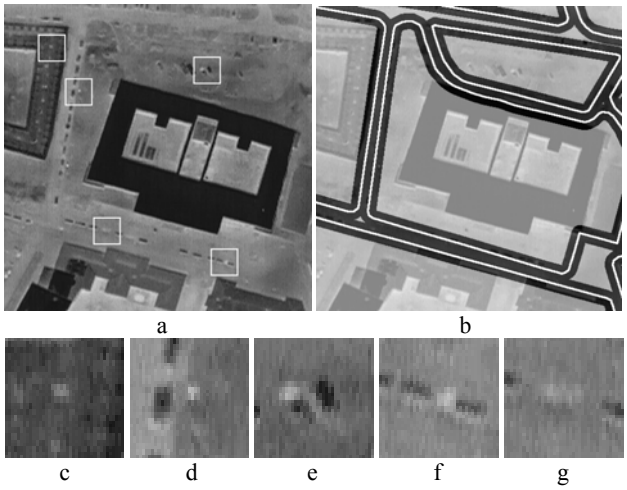

Figure 3. a) Example of a thermal IR image of an urban area. Enlargement of white frames see c-g. Parking cars appearing as dark spots which are grouped in rows along the street, b) Interest regions superimposed by a map on the IR-image, c) hot spot of a chimney, d) hot spot of a street light, e)-f) parking cars, one arrived recently arrived, g) car moved away

3.2 Detection of single vehicles

Stationary passive cars appear as dark stationary spots, because they are colder than the surrounding. They will usually occur along the margin of roads or in parking lots, and they will be grouped into rows. Fig. 3a shows such a situation. Active vehicles will appear as moving bright spots on the roads. A stationary bright spot within a row of stationary dark spots can be interpreted as a car that is still warm (has been moved short time before)(Fig. 3e,f) or as warm spot on the bare concrete giving the hint, that there has been a vehicle short time before, that moved away (Fig. 3g). Rows of bright spots in the roads are probably cars, which are waiting at a traffic light or in a traffic jam. Thus the percentage of bright versus dark spots gives a good estimation of the activity of cars in the scene. Fig. 3a shows a typical example of a thermal image of an urban site with rather low car activity. While some buildings and cars have good contrast to the background, roads do not necessarily have clear margins in this kind of imagery.

3.3 Exploiting context

Cars tend to be placed in equidistantly spaced rows along the margin of roads. This criterion allows discrimination from other spot-shaped objects. Grouping of such spots into rows of arbitrary length is a generic operation. Fig. 4a shows a section of an IR image containing a row of cars.

All detected warm and cold spots in this section are displayed in Fig. 4b. Spots caused by cars constitute only a subset of these. Fig. 4c shows those spots, that are sufficiently close to a road margin. The grouping starts only from spots which exceed a minimal mass. The grouping direction is constrained by the road margin. Only spots fitting into the straight and equidistantly spaced row model are grouped.

Still, there may be several alternatives of grouping, e.g. if two spots are close to one another in a location consistent with the model (see Fig. 4c, most right member of the row). Among the alternatives one group is selected based on an assessment, which is calculated from the number of spots, total mass, regularity in spacing and straightness and consistency in orientation of the spots. Fig. 4d shows the best group containing seven spots.

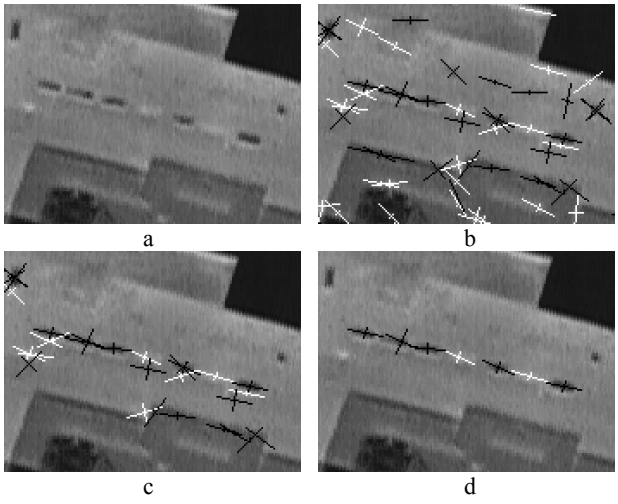

Figure 4. The benefit of grouping: a) A section of an IR-image; b) all spots constructed in that region; c) spots in the interest region given by fusion with the map; d) car-spots remaining consistent with the row model after grouping.

4. SAR DATA

Active synthetic aperture radar (SAR) sensors are independent of the time of day. The large signal wavelength in the order of centimetres provides near insensitivity to weather conditions. The increasing resolution of SAR data offers the possibility to utilize this data for detailed scene interpretations in urban areas.

4.1 Related work

Approaches for monitoring traffic have been proposed for both spaceborne systems, e.g. RADARSAT-2 [Livingstone et al., 2002], Shuttle Radar Topography Mission SRTM [Breit et al., 2003] and airborne systems, e.g. [Ender, 1999], [Eckart et al., 2000]. The moving target indication (MTI) requires vehicle detection in the SAR data and parameter estimation. Target detection and estimation can be performed either incoherently with a single SAR sensor, e.g. [Kirscht, 1998], [Livingstone et al., 2002], or coherently (along-track Interferometry), with much higher fidelity, with two [Gierull & Sikaneta, 2003] or more apertures [Ender, 1998].

For processing a SAR image from a single aperture all scene objects will be assumed stationary. The relative motion between sensor and scene causes a Doppler frequency shift, which is exploited to achieve a high azimuth resolution and to determine the correct azimuthal position of objects. The movement of objects causes artefacts. The radial velocity component of the movement leads to an azimuthal displacement (because of the additional Doppler frequency shift), the parallel component leads to blurring. This first effect can be observed in Fig. 5 comparing a SAR image and an aerial image acquired simultaneously. A cargo ship entering a lock (motion from left to right = in range direction) is mapped on the ground in the SAR image.

a b

Figure 5. Azimuth displacement of a cargo ship entering a lock. a) SAR image, b) aerial image

4.2 Detection of single vehicles

Some image based approaches exploit this azimuth displacement of detected vehicles from the expected position to estimate the radial velocity component relative to the carrier. Using the information about geometry of the route they try to derive the velocity of a vehicle. One-channel implementations may register only fast transverse or parallel movements.

Other approaches exploit SAR data from two or more channels resulting from several antennas or subapertures oriented in the direction of flight which observe the same scene at different times. A coherent processing of the data allows calculation of along-track interferograms showing moving objects by phase differences. Introducing knowledge, (e.g. typical size or shape) moving objects can be detected in the interferogram by model-based image analysis [Schulz et al., 2003].

SAR-MTI (moving target indication) processing has shown promising results in rural and suburban area. Figure 6 shows an example of a SAR-MTI result which depicts an Autobahn exit and automatically determined positions of vehicles after complete MTI processing including clutter suppression, moving target detection, high-precision azimuth position estimation and target tracking [Ender, 1999]

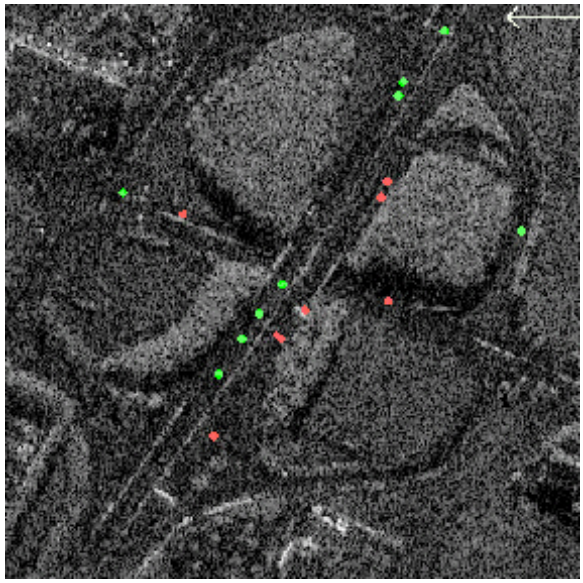

Figure 6. SAR-MTI result after target tracking (Autobahn exit Ingolstadt/Nord) [Ender, 1999]

4.3 Exploiting context

However, in urban areas SAR specific illumination phenomena like foreshortening, layover, shadow, and multipath-propagation burden the interpretation. The so-called layover phenomenon occurs at locations with a steep elevation gradient facing towards the sensor, like vertical building walls. Because object areas located at different positions have the same distance to the sensor, like roofs, walls and the ground in front of buildings, the backscatter is integrated into the same range cell. In general, the signal mixture cannot be resolved from a single SAR acquisition. The signal contributions of different objects inside a resolution cell can be separated using e.g. full polarimetric or interferometric SAR data or even a combination of both [Guillaso et al. 2003]. Layover areas appear bright in the SAR image (see Fig. 8b). Perpendicular alignment of buildings to the sensor leads to strong signal responses by double-bounce at the dihedral corner reflector between the ground and the building wall. All these double-bounce signals have the same time-of-flight. This results in a line of bright scattering in the azimuthal direction at the building footprint.

At the opposite building side, the ground is partly occluded from the building. This region appears dark in the SAR image, because no signal returns into the related range bins.
Layover and radar shadow (e.g. caused by tall buildings) may hinder the visibility of neighboured objects of interest, like roads. The sizes of the layover areas l_g and shadow areas s_g on the ground in range direction (see Fig. 7) depend on the viewing angle θ and the building height h.

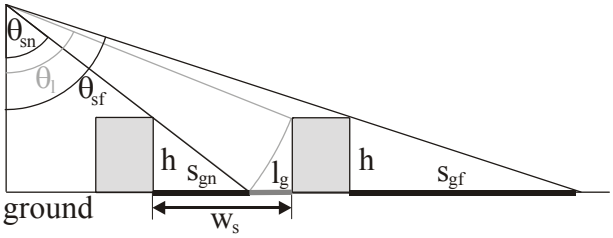

c

Figure 7. Shadow and Layover from buildings displaced in range direction.

The viewing angle increases in range direction over the swath. Assuming a range of the viewing angle θ between 40° and 60°, the shadow length of a certain building is more than doubled from near to far range. In Fig. 7 such a situation is depicted (shadow length s_{gn}, s_{gf}). A worst case will arise if a road between two building rows is oriented parallel to the sensor trajectory. The street is partly occluded from shadow and partly covered with layover. An object on the road can only be sensed undistorted, if a condition for the road width w_S holds:

$$w_s > s_{gn} + l = h \cdot (\tan(\theta_{sn}) + \cot(\theta_l)). \quad (1)$$

In the sketch (Fig. 7) the angles θsn and θsf vary remarkably between the two buildings. In reality the angle changes only slightly over the width of a road. Hence, for the estimate of the size of the problem areas a constant angle ($\theta sn = \theta sf$) is assumed. An angle of 55° in both cases and a building height of 20m give a minimum w_S of 40m.

4.4 Simulation of shadow and layover

It is essential to determine a-priori the optimal SAR acquisition parameters in order to minimize the influence of layover and shadow for a selected area of interest or an object class. For this purpose, maps and high-resolution elevation data from a GIS are required [Soergel et al., 2003b].

Based on a DEM, layover and shadow regions are simulated [Meier et al, 1993]. From the sensor position, the DEM grid is sampled in range direction. Layover and shadow regions are detected analyzing the distance and the viewing angle. By intersection of these results with the map data, the affected areas of buildings and roads are identified

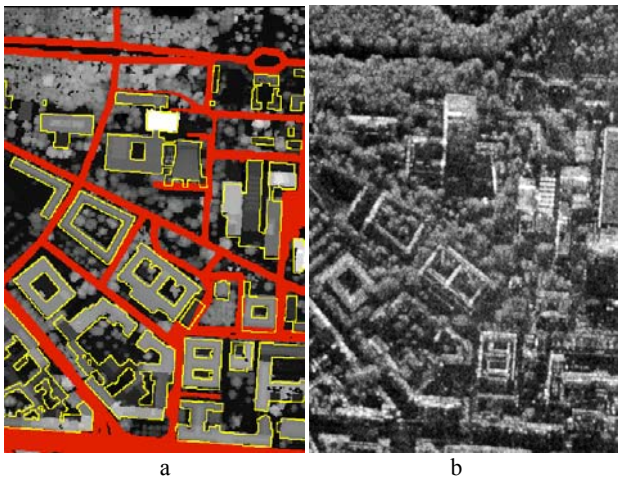

a b

Figure 8. a) LIDAR DEM superimposed with the layers of buildings (yellow) and roads (red). b) SAR image

.A simulation of shadow and layover areas with the given SAR parameters is shown in Fig. 9a. The results are given in Table 1. The large viewing angle suggests a larger portion of shadow compared to layover. This would be the case if all objects in the scene were detached, their signals not interfering with each other. However, in the test scene, the ground distance in range direction between the objects is often small. This results in many mixed pixels where shadow and layover are both present. Less than 20% of the road area can be sensed undisturbed.

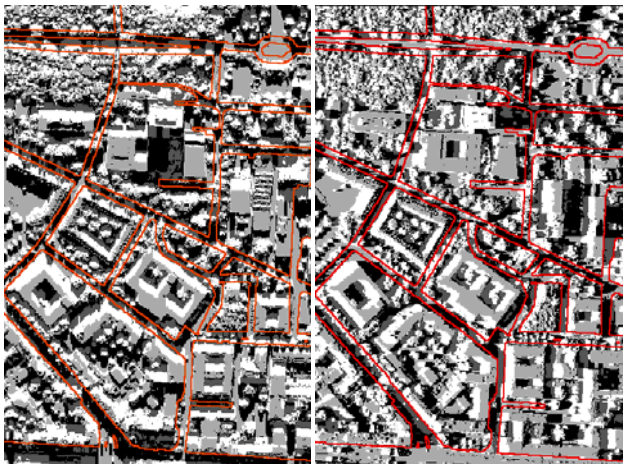

a b

Figure 9. Simulation results for given SAR parameters from Fig 8b. (layover: white, shadow: black, layover+shadow: dark gray, reliable: bright gray). a) illumination from north (top), b) illumination from west (left).

4.5 Determination of optimal aspect and viewing angles

In order to estimate the optimal aspect and viewing angles for an arbitrary SAR measurement a large number of simulations have been carried out. Fig. 9b shows the result for a simulated illumination of westward aspect direction. The aspect angle was altered systematically in steps of 5°. For each of the 72 aspect directions the layover and shadow areas were detected for 9 different viewing angles. The viewing angle θ was chosen between 30° and 70° with 5° increment. This results in 648 simulations. From this set, the best single SAR illumination direction was determined. The results are shown in Table 1.

Parameters	given			optimal	
Area	Complete	Roads	Roofs	Roads	Roofs
Shadow	28	39	16	27	14
Layover	25	19	34	16	28
Mixed	19	24	7.5	19	7
Reliable	28	20	43	39	52

Table 1. Results (in %) of shadow/layover detection for given (see Fig 8b) and optimal SAR parameters

The optimal illumination direction with respect of the visibility of buildings was from the east with a viewing angle of 60°. More than half of the roof area would be visible in SAR data acquired with these parameters. In the case of the roads, the best result is achievable for an illumination from exactly north with a viewing angle of 45°. This direction coincides with one main road orientation.

4.6 Fusion of SAR data from different views

Starting from the already found best SAR illumination the remaining set of simulations is scanned for the best complementing SAR measurement. Again, the portion of useful data from the object class of interest is maximized. This means that the objects have to be visible from at least one viewpoint. The procedure is repeated twice based on the result of the previous step. The analysis is carried out independently for the object classes buildings and roads. The benefit for a fusion of 2, 3, and 4 SAR acquisitions can be seen in Table 2.

SAR measurements	1	2	3	4
Roof area (undistorted)	52	73	82	87
Road area (undistorted)	39	47	56	62
Road area (shadow)	27	10	4	2

Table 2. Portion (in %) of visible roof and road area for the optimal single and set of several SAR acquisitions

5. DISCUSSION

5.1 Optical data

The detection algorithm was tested on a series of high resolution aerial images (ca. 15cm ground resolution) of complex downtown areas. No preclassification of regions of interest had been carried out. It shows that the vehicle detection achieves a high correctness of 87% but only a moderate completeness of 60%. This is a clear consequence of the stringent parametric model. In contrast, the (independently run) queue detection reaches a higher completeness of 83%, however, as can be anticipated from the weaker generic queue model, the correctness is below 50%. The effect of fusion and recovering missed extractions increases the completeness up to 79% while the correctness is almost the same as for the vehicle detection.

Failures occur in regions where the complete road is darkened by building shadows. This could be overcome by pre-classifying shadow regions, so that the vehicle model can be adapted accordingly. Further improvements, mainly regarding the vehicle detection scheme, include the optional incorporation of true-colour features and the use of a model hierarchy and/or geometrically flexible models similar to Olson et al. [1996] and Dubuisson-Jolly et al. [1996]. The use of multi-view imagery to separate moving from parking vehicles and to estimate vehicle velocity would be another avenue of research.

5.2 Infrared data

A comparison of data sets recorded at different time of day, weather condition, and temperature has shown that the appearance of roads and vehicles in images differ significantly. For detection of stationary cars the vehicle model has to consider the different illumination and temperature situations. Subject of future work will be the modelling of vehicles under consideration of the different data statistics.

5.3 InSAR data

The analysis of buildings and roads in urban areas is limited due to the SAR sensor principle. With a single SAR measurement useful data can be acquired usually for a minor part of the object areas only. It was shown that this limitation can be overcome by taking additional SAR data from different aspect and viewing angles into account. In case of the roads the best result is achievable for an illumination from exactly north and west with a viewing angle of 45°. These directions coincide with the main road orientations. The third illumination direction is along the tilted long road from 210° anti-clockwise towards north (off nadir angle $\theta = 50°$) and the fourth from east to west ($\theta = 60°$). However, even in the case of the fusion of four SAR images still more than a third of the road area can not be sensed without distortions. Assuming the layover problem might be resolved using techniques of SAR Polarimetry and/or Interferometry, it is worthwhile to focus on the shadow areas alone. In the last row of Table 2 it is shown that only 10% of the road area would be occluded combining two carefully chosen SAR acquisitions.

6. CONCLUSION

Due to the high resolution of the used optical data a detailed three-dimensional modelling of vehicles was suitable and powerful for discrimination of these objects from other objects of the scene. The recognition is supported by utilizing the illumination situation and analysis of the shadow which is important in case of low contrast between vehicle and road surface. Exploiting context information by analysis of vehicle queues increases the reliability of recognition. In the presented approach map information was not utilized, but can easily be incorporated. Analysis of monocular data allows an assessment regarding movement or activity of vehicle only indirectly by assignment of vehicles to traffic lanes or parking space.

Particularly at night thermal infrared sensors yields suitable data for traffic monitoring. The used images of the video had a lower resolution than the aerial imagery. Vehicles have to be modelled as elongated blobs. Because of the simple model, context knowledge from maps and about parking structure was exploited to achieve a reasonable discrimination of vehicles from other objects of the urban scene. Thermal images allow the analysis of recently moved vehicles.

SAR sensors systems are able to monitor urban scenes day and night and almost independent from weather. In contrast to the visible and infrared imagery which was taken in nadir view SAR imagery has to be taken in oblique view which is an inherent part of the sensor principle. Due to this fact in urban areas streets close to buildings or between buildings may be partially invisible or distorted by layover. However, the side-looking illumination by SAR causes inherent artefacts particularly in dense urban areas. An analysis of multi-aspect SAR data offers an improvement of the results. The SAR acquisition directions can be locally optimized based on DEM and map data of a GIS.

REFERENCES

Breit H, Eineder M, Holzner J, Runge H, Bamler R (2003) Traffic monitoring using SRTM along-track interferometry. IEEE

Dreschler L, Nagel HH (1982) Volumetric model and trajectory of a moving car derived from monocular TV frame sequence of a street scene. CGIP, 20:199-228

Dubuisson-Jolly MP, Lakshmanan S, Jain A (1996) Vehicle segmentation and classification using deformable templates. IEEE PAMI, 18 (3): 293–308

Eckart O, Rombach M, Holz A, Hofmann C, Schwaebisch M (2000) Traffic monitoring using along track airborne interferometric SAR systems. ITS-Congress, Turin

Ender JHG (1998) Experimental results achieved with the airborne multi-channel SAR system AER-II. Proc. EUSAR'98, 315-318.

Ender JHG (1999) Space-time processing for multichannel synthetic aperture radar. IEE Electr. and Comm. Engineering J., 29-38

Guillaso S, Ferro-Famil L, Reigber A, Pottier E (2003) Urban Area Analysis Based on ESPRIT/MUSIC Methods using Polarimetric Interferometric SAR. 2nd GRSS/ISPRS Joint workshop on remote sensing and data fusion on urban areas, URBAN 2003. IEEE, 77-81.

Gierull CH, Sikaneta IC (2003) Raw data based two-aperture SAR ground moving target indication. IGARSS 2003 (IEEE) Vol II:1032-1034

Gorte B, van Zuylen H, Hoogendoorn S (2002) Opstellen meetsysteem dataverzameling congestie. Technical report. TU Delft, The Netherlands

Haag M, Nagel HH (1999) Combination of edge element and optical flow estimates for 3D-model-based vehicle tracking in traffic sequences. IJCV, 35 (3): 295–319

Hinz S, Baumgartner A (2001) Vehicle detection in aerial images using generic features, grouping and context. In: Radig B, Florczyk S (eds) Pattern recognition, DAGM 2001, LNCS 2191, Berlin:Springer, 45-52

Hinz S (2004) Detection of vehicles and vehicle queues in high resolution aerial images. Photogrammetrie, Fernerkundung, Geoinformation (in press)

Kirscht M (1998) Detection, Velocity Estimation and Imaging of Moving Targets with Single-Channel SAR, EUSAR`98, 587-590.

Livingstone CE, Sikaneta I, Gierull CH, Chiu S, Beaudoin A, Campbell J, Beaudoin J, Gong S, Knight TA (2002) An airborne sysnthetic aperture radar (SAR) experiment to support RADARSAT-2 ground moving target indication (GMTI). Can. J. Remote Sensing 28(6): 794-813

Liu G, Gong L, Haralick R (1999) Vehicle detection in aerial imagery and performance evaluation. ISL-Technical Report, Intelligent Systems Laboratory, University of Washington, Seattle, WA.

Meier E, Frei U, and Nuesch D (1993) Precise Terrain Corrected Geocoded Images. In: Schreier G (ed.) SAR Geocoding: Data and Systems. Karlsruhe: Wichmann, 173-185

Michaelsen E, Stilla U (2000): Ansichtenbasierte Erkennung von Fahrzeugen. In: Mustererkennung. DAGM 2000, Berlin: Springer 245–252.

Michaelsen E, Stilla U (2001) Estimating urban activity on high-resolution thermal image sequences aided by large-scale vector maps. In: IEEE/ISPRS Joint Workshop URBAN´01, 25-29.

Moon H, Chellappa R, Rosenfeld A (2002) Performance analysis of a simple vehicle detection algorithm. Image and Vision Computing, 20 (1): 1–13

Papageorgiou C, Poggio T (2000) A trainable system for object detection. International Journal of Computer Vision, 38 (1): 15–33.

Partsinevelos P, Agouris P, Stefanidis A (2000) Modelling movement relations in dynamic urban scenes. *International archives of photogrammetry and remote sensing*. Vol. 33, part B4, 818-825

Quint F (1996) Recognition of structured objects in monocular aerial images using context information. In: Leberl F, Kalliany R, Gruber M (eds) Mapping buildings, roads and other man-made structures from images. Wien: Oldenburg, 213-228

Rajagopalan A, Burlina P, Chellappa R (1999) Higher-order statistical learning for vehicle detection in images. International Conference on Computer Vision.

Ruskoné R, Guiges L, Airault S, Jamet O (1996) Vehicle Detection on Aerial Images: A Structural Approach. 13th International Conference on Pattern Recognition.

Schneiderman H, Kanade T (2000) A Statistical Method for 3D Object Detection A-plied to Faces and Cars. Computer Vision and Pattern Recognition.

Schulz K, Soergel U, Thoennessen U, Stilla U (2003) Elimination of across-track phase components in airborne along-track interferometry data to improve object velocity measures. IGARSS 2003, IEEE

Soergel U, Thoennessen U, Stilla U (2003a) Visibility analysis of man-made objects in SAR images. 2nd GRSS/ISPRS Joint workshop on remote sensing and data fusion on urban areas, URBAN 2003. IEEE, 120-124

Soergel U, Thoennessen U, Stilla U (2003b) SAR data acquisition for event-driven mapping of urban areas using GIS. GeoBIT/GIS Journal for spatial information and decision making (12):32-37.

Stilla U, Soergel U, Thoennessen U (2003) Potential and limits of InSAR data for building reconstruction in built up-areas. ISPRS Journal of Photogrammetry and Remote Sensing, 58(1-2):113-123

Sujew S, Ernst I (2003) LUMOS: Airborne traffic monitoring. In: Ruhe M (ed) International workshop on airborne traffic monitoring. DLR

Tan T, Sullivan G, Baker K (1998) Model-Based Localisation and Recognition of Road Vehicles. International Journal of Computer Vision, 27 (1): 5–25.

Toth CK, Barsi A, Lovas T (2003) Vehicle recognition from LIDAR data. *International archives of photogrammetry and remote sensing*. Vol. 34, part 3/W13:

Wolffe WL, Zissis GJ (1985) The infrared handbook. Infrared Information Analysis (IRIA) Center, Environmental Research Inst. of Michigan

Zhao, Nevatia, R (2001) Car detection in low resolution aerial image. International Conference on Computer Vision.